Case Studies in Construction Materials 18 (2023) e01819

Contents lists available at ScienceDirect

Case Studies in Construction Materials

journal homepage: www.elsevier.com/locate/cscm

Case study

In-plane shear behaviour of prefabricated modular wall system assembled of fibre reinforced polymer composites

Arvind Sharda [a], Allan Manalo [a], Wahid Ferdous [a,*], Yu Bai [b], Lachlan Nicol [c], Ali Mohammed [c], Brahim Benmokrane [d]

[a] *University of Southern Queensland, Centre for Future Materials (CFM), School of Engineering, QLD 4350, Australia*
[b] *Department of Civil Engineering, Monash University, Clayton, VIC 3800, Australia*
[c] *Wagners Composite Fibre Technologies (CFT), Wellcamp, QLD 4350, Australia*
[d] *University of Sherbrooke, Research Center on FRP Composite Materials (CRUSMaC), Department of Civil & Building Engineering, Sherbrooke, Quebec J1K 2R1, Canada*

A R T I C L E I N F O

Keywords:
Composite wall system
Connection
In-plane shear load
Modular construction
Single and double frame

A B S T R A C T

Fibre reinforced polymer (FRP) composites could be an alternative of traditional materials for modular construction due to their superior strength to weight ratio, corrosion resistance and immunity from biological degradation. This paper investigates the in-plane shearing behaviour of full-scale modular wall system made from all glass FRP (GFRP) rectangular hollow section (RHS) frames and GFRP sheathing. Monotonic in-plane shear load was applied to understand the effect of important parameters such as sheathing height offset from bottom of wall panel, wall opening, customised angle brackets for additional shear resistance, and comparison between single and double frame wall system. The results show that the wall panel with 10 mm sheathing offset from bottom deformed under shear and avoided high compression stress with significant higher loading capacity than panel with full sheathing. The stiffness of wall panel with opening can be estimated from the wall opening ratio of opening to total wall area. Furthermore, the installation of customised angle brackets can improve the loading capacity and stiffness of the wall panel. Finally, high height-to-width panel aspect ratio increased the loading capacity but reduced the overall panel stiffness in both single and double wall panels. Overall, this study presented that the structural parameters alter the ultimate failure modes which increased the overall loading capacity and impacted the panel stiffness.

1. Introduction

Modular construction is increasingly adopted in industry nowadays, with a few major benefits of high quality, quick construction, and lower cost of construction over traditional on-site constructions [1–5]. Ferdous et al. [1] presented a number of examples of modular systems for two- to 44-storeys high buildings, wherein timber, steel, concrete and their hybrid materials are used as

* Correspondence to: University of Southern Queensland, Centre for Future Materials (CFM), School of Engineering, Toowoomba, QLD 4350, Australia.

E-mail addresses: Arvind.Sharda@usq.edu.au (A. Sharda), Allan.Manalo@usq.edu.au (A. Manalo), Wahid.Ferdous@usq.edu.au (W. Ferdous), Yu.Bai@monash.edu (Y. Bai), Lachlan.Nicol@wagner.com.au (L. Nicol), ali.mohammed@wagner.com.au (A. Mohammed), Brahim.Benmokrane@USherbrooke.ca (B. Benmokrane).

https://doi.org/10.1016/j.cscm.2022.e01819
Received 10 October 2022; Received in revised form 23 December 2022; Accepted 29 December 2022
Available online 30 December 2022

Table 1
Mechanical properties of the GFRP sheeting and M20 Bolts.

Properties	Test Standard	GFRP Sheet		RHS Profile [37]		M20 Bolts [37]
		Avg. Value	Avg. SD	Avg. Value	Avg. SD	Avg. Value
Longitudinal tensile strength (MPa)	ISO 527–1:1995 [38]	568	1.9	686	44.2	-
Longitudinal tensile elastic modulus (GPa)		33.8	1.9	42.9	2.2	-
Longitudinal Poisson's ratio		0.27	0.01	0.30	0.02	-
Transverse tensile strength (MPa)		42	1.2	47	3.9	-
Transverse tensile elastic modulus (GPa)		11.7	0.3	12.1	1.1	-
Transverse Poisson ratio		0.13	0.03	0.15	0.07	-
Longitudinal flexural strength (MPa)	ISO 14125:199 [39]	689	0.4	-	-	-
Longitudinal flexural elastic modulus (GPa)		26.4	1.1	-	-	-
Transverse flexural strength (MPa)		61	2.1	-	-	-
Transverse flexural elastic modulus (GPa)		9.1	0.1	-	-	-
In-plane shear strength (MPa)	ASTM D5379:1993 [40]	69	2.5	89	14.6	-
Longitudinal interlaminar shear strength (MPa)	ASTM D2344–16 [41]	37	0.9	-	-	-
Transverse interlaminar shear strength (MPa)		9	0.6	-	-	-
Minimum tensile strength (MPa)	Property class: 8.8, M20, Pitch 2.5 mm, Minor diameter 19.67 mm	-	-	-	-	830
Proof strength (MPa)		-	-	-	-	600
Minimum yield strength (MPa)		-	-	-	-	660
Minimum shear strength (MPa)		-	-	-	-	514.6

construction material. Whereas, researchers proposed to utilise the glass fibre reinforced polymer (GFRP) composites over the conventional construction material due to the superior physical properties such as high strength to weight ratio, immunity to corrosion, immunity to pest decay and biological decay [6,7]. The applications of GFRP as reinforcement in concrete [8,9], strengthening of masonry walls [10,11] and repairing of existing structures [12,13] are widely investigated. In building construction, walls may be subjected to compression, bending and in-plane shear load for example caused by dead load and wind. While the applications of GFRP panels under axial compression [14,15] and flexural loading are explored in literature [16–19], the effect of in-plane shear load on all composite wall panels is not well understood and requires more investigations for their potential and safe application.

The behaviour of modular composite wall systems under in-plane shear was studied in [20], where adhesively bonded frames were developed for in-plane shear load, with full length sheathing composite panel connected from bottom plate or full height tie down bolts. It was found that the failure was initiated by the diagonal cracking in magnesium oxide (MgO) board in both panels. Under shear load, the far side of panel sheathing experienced compression load due to the ground contact. This phenomenon may intensify the stress in sheathing to cause earlier cracking in sheathing. Similar phenomenon may cause the earlier fastener bending and fastener pull off under in plane shear load for timber walls [21–23], tearing thin plate around fasteners [24] and local sheet buckling near to compression stud in steel concrete walls [25–27]. This type of failure can be avoided by shortening the length of sheathing from the bottom in composite shear wall. It is important therefore to understand the effect of sheathing height offset from the bottom of wall panel under in-plane shear load.

Wall openings are found as an important feature in building structures and also reduces the stiffness and introduces stress concentration at edges [28]. A number of studies has been conducted on in-plane shear behaviour on traditional wall panels with openings, where it is reported that inclined shear cracking at corner is a common failure behaviour in timber [29,30] and concrete [31,32] shear walls due to high stress concentration at opening corners. However, Husain [33] mentioned that use of fibre composites in retrofitting at wall openings helps to increase the loading capacity of the wall panel but has a minor effect on the wall stiffness. Very few studies were conducted for in-plane shear behaviour on composite wall systems manufactured by full pultruded panel section [34]. This can limit the development of such composite wall system for modular construction. Therefore, wall systems made of assembly of multiaxial pultruded GFRP rectangular hollow section (RHS) adhesively bonded to GFRP sheathing may be of interest and their performances under in-plane shear load with and without wall openings need to be understood.

In modular structures, connections between structural members ensure the overall structural integrity. Several studies have been conducted on the connections between composite frame and sheathing [14–18,35] and their failure mechanisms are explored. Under in-plane shear loading, however, the connection between composite wall frame members and connection between frame with other module or ground is very important. Angle brackets [36] and hold-down [30] are commonly used to resist shearing and uplift during in-plane loading respectively for timber shear walls. Application of nails in wooden wall panels also ease the fabrication and installation of angel brackets and hold downs. In all composite wall panels, however, nail application is difficult to implement and therefore angle brackets and hold downs are usually riveted with the frame member. In a previous study of all composite wall panels [14] under axial compression, it was highlighted that failure was mainly governed by the delamination of sheathing and had a minimal or negligible effect on riveted angle brackets because overall load was carried by the frame and sheathing. This indicates the potential

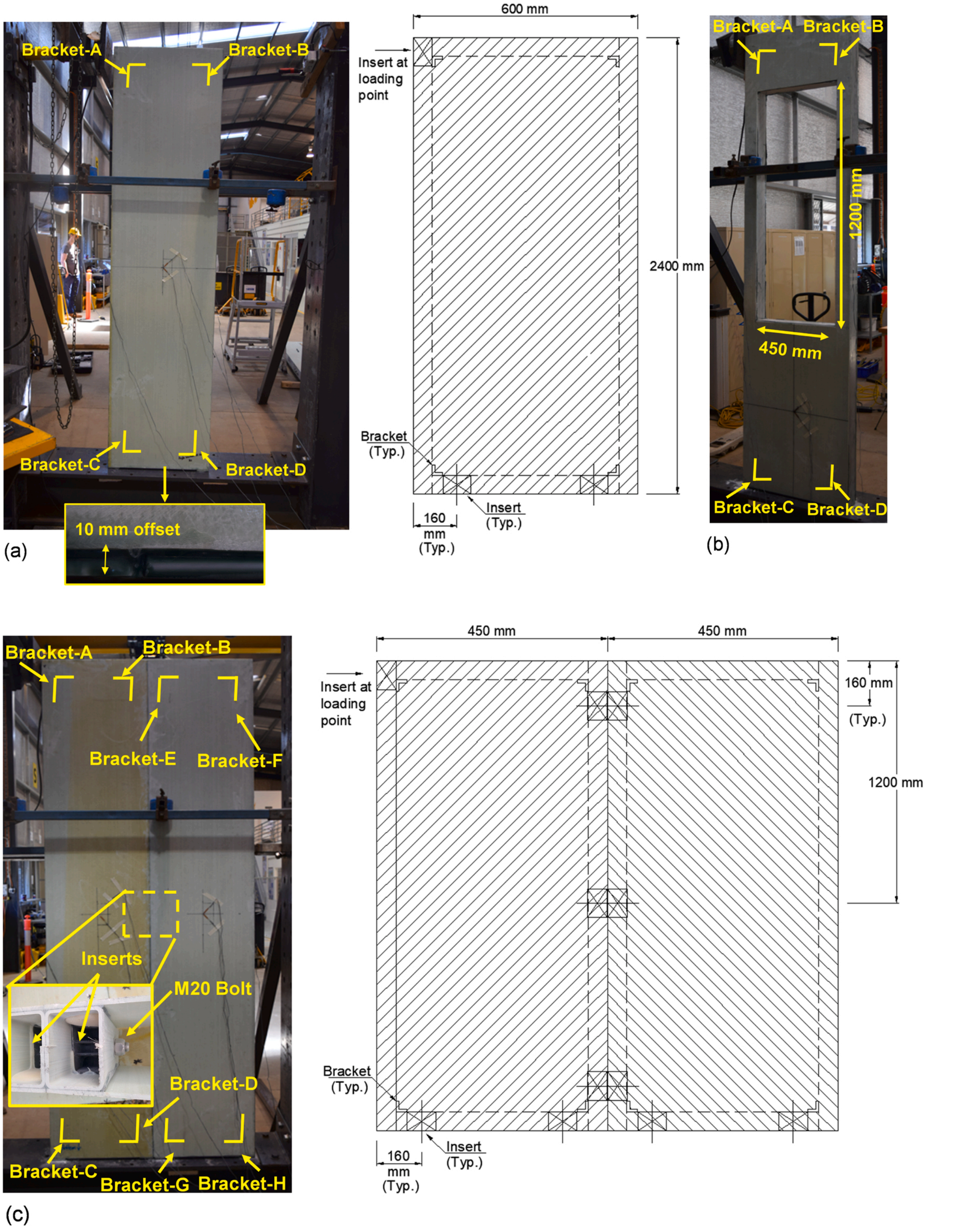

Fig. 1. (a) Single frame (b) Panel with opening (c) Double wall frame.

usage of riveted angle bracket for composite wall system under compression. The applications of riveted angle brackets and hold-down under in-plane shear load are however not explored for shear resistance and therefore further investigation is required. Manalo [20] tested a double frame composite wall panels connected with shear key that helps to transfer the load from one panel to another, hence double frame achieved twice stiffness and loading capacity of single frame. In addition, bolted joints are convenient to join two wall

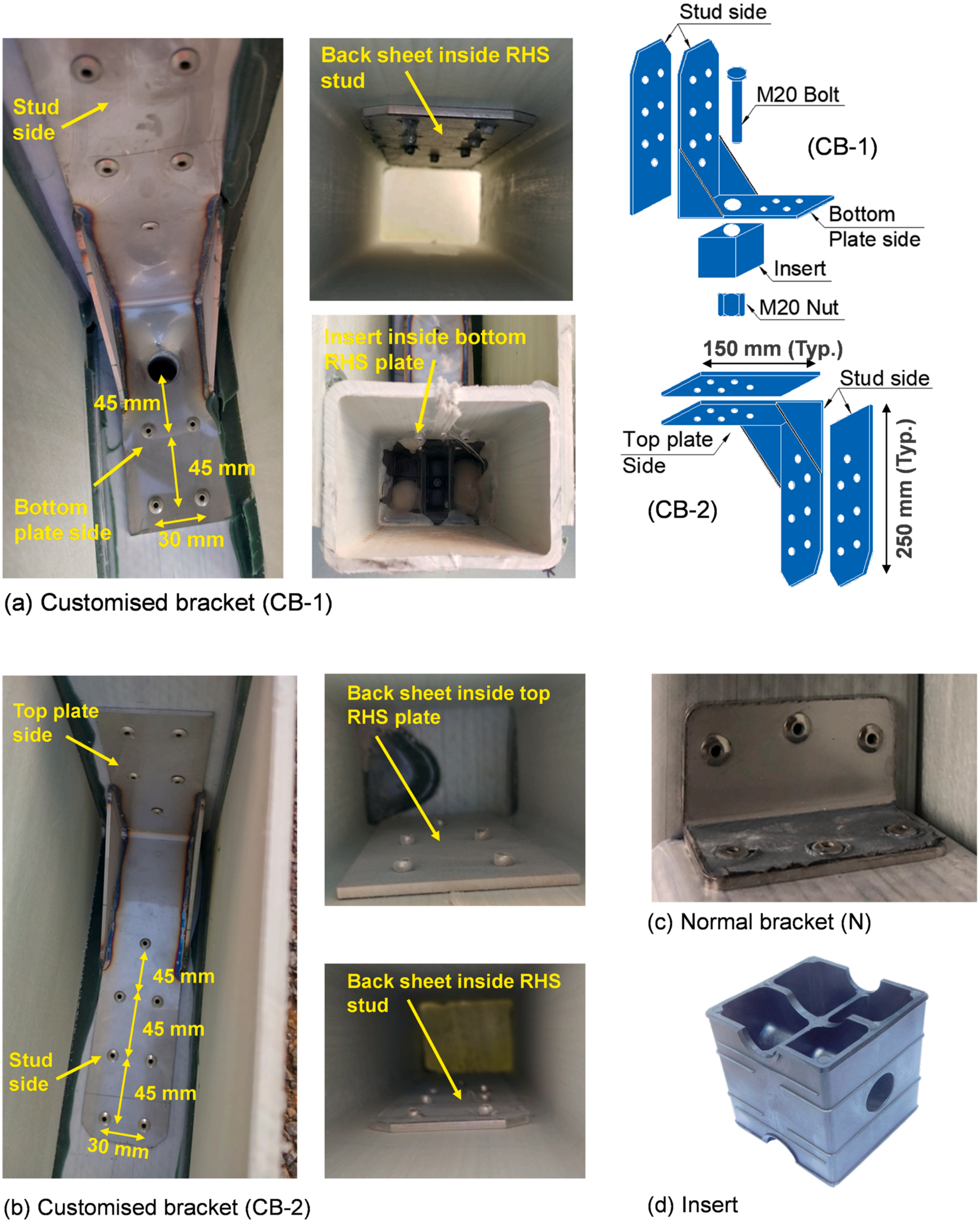

Fig. 2. (a), (b) and (c) Details of angle brackets used in composite wall panels (d) Anti-crush insert [43].

panels together but their performance and behaviour under in-plane shear load needs to be investigated.

In this study, GFRP composite wall panels were manufactured and tested under in-plane shear load. The novelty of this study is that it analyses the behaviour of key design parameters, such as effect of sheathing height from the bottom of wall panel, effect of wall opening in composite wall, effect of angle brackets and comparison of single and double frame composite wall under in-plane shear load. The results of this study may provide a better understanding of in-plane shear behaviour of modular composite wall systems with these key parameters for their reliable design and application.

2. Experimental programme

2.1. Materials

A pultruded GFRP rectangular hollow section (RHS) of 100 × 75 × 5 mm was used to fabricate the main frame of the wall panels. The material properties of the RHS profile were taken from past research [37] where the same materials were evaluated as used in this study, and are listed in Table 1. Multiaxial 6 mm thick GFRP sheet was used on both sides as a sheathing for all the wall panels. The relevant ASTM and ISO test standards using coupon specimens were followed to evaluate the mechanical properties of the sheathing material and are summarised with standard deviation (SD) in Table 1.

2.2. Specimen details

Six full-scale wall panels were fabricated by industrial partner to maintain high quality fabrication and tested under in-plane shear. Stainless-steel (SS) angle brackets measuring 35 × 35 × 70 mm were used to connect the RHS studs and plates to form a main frame for the panels; the sheathing was adhesively bonded to the frames similar to that in Fig. 1(a) and in [14]. All wall panels were 2400 mm in height and single frame panels were 600 mm wide. One panel with window opening 450 mm x 1200 mm was fabricated to compare with full sheathed panel in Fig. 1(b). Two 450 mm wide single-frame panels were connected with M20 bolts to fabricate the double-frame wall panels shown in Fig. 1(c). Customised angle brackets in Fig. 2(a) and (b) are used in three wall panels as in Table 2. Inserts in Fig. 2(d) were provided at loading point, bolted inter-panel and bottom connections to prevent any stress concentration; the bolts were tightened to a torque of 20 N-m as recommended by Manalo et al. [42]. The panels are designated according to the number of panels (F for single frame and DF for double walls), effect of sheet offset from the bottom (S_0 and S_{10} for full sheet and 10 mm short from the bottom respectively), effect of window opening (O) and effect of customised angle brackets (B_2 and B_4, for two or four angle brackets respectively). For example, specimen $FS_{10}O$ is a single wall with the sheathing 10 mm short from the bottom with window opening, while specimen $FS_{10}B_2$ is a single wall panel with the sheathing 10 mm short from the bottom with two customised angle brackets.

2.3. Test setup and instrumentation

All wall panels are installed upright on the UB460 steel beam by using M20 bolts and tested under monotonic in-plane shear load applied by 100 kN hydraulic jack from the top left corner according to the procedure in ASTM E72–05 [44] and in Fig. 3(a). Axial load is not considered as recommended by [45]. One full scale wall panel per parameter was tested similar to previous research [15,18,35], however, this may limit the repeatability of the results. Therefore, variety of instruments were attached to capture data from critical locations. 20 mm uniaxial strain gauges (SG) capacity were used to measure strains at the locations (see Section 3). As shown in Fig. 3 (a), string pot is connected to the right top corner to measure lateral deflection, 30-ton capacity of load cell was attached to hydraulic jack to record applied load and digital image correlation (DIC) camera was used to record lateral deflection at various points of wall panel along the height in Fig. 3(b). Strain, load, and deflection data were recorded in a SmartStrain data logger system. Roller supports on both sides were provided to avoid falling and maintain the vertical alignment.

3. Experimental results and discussion

Failure modes of all wall panels are summarised in Fig. 4 and summary of experimental results is summarised in Table 3. In general, failure originated at the bottom plate with longitudinal cracking in the RHS section or delamination between the sheathing and bottom plate. The effects of various parameters are discussed in below sections.

3.1. Effect of sheet offset

The effect of sheathing offset was evaluated by comparing the FS_{10} (10 mm short sheathing length from the bottom plate) and FS_0 (Full panel height sheathing length). The overall results show that a higher in-plane shear capacity can be achieved by shortening the

Table 2
Angle bracket details.

Panel Label	Bracket-A	Bracket-B	Bracket-C	Bracket-D
FS_0	N	N	N	N
FS_{10}	N	N	N	N
$FS_{10}O$	N	N	N	N
$FS_{10}B_2$	N	CB-2	CB-1	N
$FS_{10}B_4$	CB-2	CB-2	CB-1	CB-1
DFS_{10}	N	CB-2	CB-1	N
	Bracket-E	Bracket-F	Bracket-G	Bracket-H
DFS_{10}	N	N	N	N

(N = Normal bracket), (CB-1 Customised bracket-1), (CB-2 Customised bracket-2), For more details see Fig. 2.

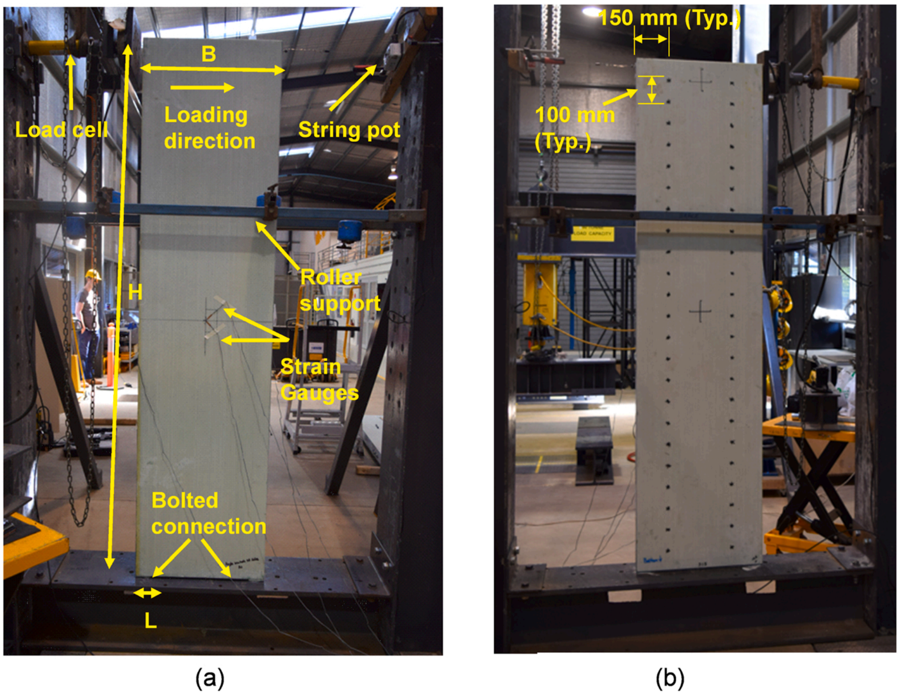

Fig. 3. (a) Test setup (b) Marking for DIC measurement.

sheathing length in the wall panel at the bottom as it changed the failure behaviour of the panel. The effect of sheet offset on load deflection, failure behaviour and load strain behaviour are discussed in the following sections.

3.1.1. Load deflection behaviour

Fig. 5 shows the load deflection behaviour of FS_{10} and FS_0 panels. The experimental results indicate that both composite panels exhibit similar shear stiffness but a significant difference in loading capacity can be observed. This is because the shortening of the sheathing height by 10 mm from bottom has a very minimal effect on the lateral stiffness of panel. Whereas it alters the failure mechanism from inter laminar delamination of sheet to transverse splitting of bottom RHS plate as explained in Section 3.1.3 that helps to eliminate premature delamination failure and consequently increase the loading capacity of wall panel. Experimental panel stiffness (K) is calculated by the ratio of linear portion of load deflection curve in Fig. 5 and recorded as 229 N/mm and 233 N/mm for FS_0 and FS_{10} respectively. By considering wall panel as a cantilever under point load, the experimental flexural stiffness of 1.05×10^{12} N/mm^2 for both panels can be calculated by Eq. (1). However, the calculated panel flexural stiffness is 1.19×10^{12} N/mm^2 by Eq. (2) and material properties in Table 1 corresponding 13.7% higher than experimental stiffness. This could be due to the theoretical analysis did not consider fabrication imperfection tolerance and/or the SD of 6–8% in material properties listed in Table 1 may have some influence. The 10 mm sheathing offset from the bottom plate in FS_{10} increased 1.71 times loading capacity than panel FS_0. The maximum loading capacity of FS_0 was 6.84 kN with horizontal deflection of 30.1 mm. Thereafter, no increment in load was observed and panel failed at 6.01 kN. Whereas FS_{10} reached to 11.6 kN loading capacity with horizontal deflection of 79.8 mm. Thereafter, a significant drop in the load can be observed. Before reaching to the peak load, both panel shows nonlinear behaviour until ultimate failure and this is explained in the following section.

$$EI = \frac{H^3 m}{3} \tag{1}$$

$$EI = 2E\left(I + Ad^2\right) \tag{2}$$

where E is the longitudinal modulus of elasticity in the longitudinal direction, I is the second moment of inertia in the direction of the applied load, H is the height of the wall panel, m is the ratio of load and deflection of linear portion of load deflection curve, A is the cross sectional area of RHS stud and d is the distance from centre of bottom bolt and the centroid of the RHS.

3.1.2. Failure behaviour

FS_0 exhibits a linear elastic behaviour until 6.1 kN load and then a loud sound was heard with a minor load drop at 6.1 and 6.3 kN. This could be due to the initiation of delamination between bottom plate and sheathing. Upon the load was reaching at 6.8 kN, a loud sound was heard followed by major delamination between sheathing and bottom RHS plate as shown in Fig. 4(a) and this caused a sudden loss of 29% load in Fig. 5. Thereafter, the panel regains 18% load because of the load transferred between angle bracket (N) and bottom plate. Upon increasing the load, a continuous creaking sound was heard that could be due to the corner splitting of RHS bottom plate in Fig. 4(b) followed by the crushing of insert in Fig. 4(c) but finally at 6.0 kN the panel failed due to the rivets pull off from bottom plate in Fig. 4(d). On the other hand, FS_{10} exhibits a linear elastic behaviour until 6.9 kN load and then a cracking sound was heard that could be due to the initiation of cracking of insert in the bottom plate in Fig. 4(I). Thereafter decrease in the shear stiffness can be observed in the panel. At 8.7 kN a sudden 6.7% load drop was observed that could be due to the major crushing of insert, because no delamination between bottom plate and sheathing was observed similar to FS_0. Then a minor increment in panel stiffness was observed but at 11.6 kN sudden drop in load with loud sound can be attributed by the splitting of bottom RHS plate in Fig. 4(g). After major crushing of the insert at 8.7 kN, the load was mainly carried by the bottom RHS plate that can be explained by the inundation of washer in Fig. 4(f). A minor crushing of vertical stud was also observed as shown in Fig. 4(h).

3.1.3. *Load strain behaviour*

Fig. 6(a), shows the load strain behaviour of FS_{10} and FS_0 wall panels. SG-1 and SG-2 of both panels are attached on the vertical studs and exhibit a linear behaviour in tension and compression. Similar load strain slopes of SG-1 and SG-2 in both panels indicate that sheathing offset does not have much impact on the load distribution on vertical studs. Similarly, SG-3 and SG-4 also exhibit linear load strain behaviour in both panels. Whereas a minor fluctuation in SG-4 of FS_{10} can be seen at 8.7 kN, which could be due to the major cracking in inserts in Fig. 4(e), because no delamination similar to FS_0 was observed. On contrary to this, SG-3 and SG-4 of FS_0 show 2.3 and 1.4 times higher strain than FS_{10}, respectively. This indicates that in FS_{10} sheathing exhibits complete shear behaviour and deformed along with panel in Fig. 6(b). Hence, strain in SG-3 and SG-4 is recorded less than SG-1 and SG-2 due to closer location to the neutral axis. Whereas, in FS_0 sheathing experienced combination of shear and high compression stress concentration at compression side bottom corner, due to contact between sheathing and UB460 in Fig. 6(c). Hence the strain in SG-3 and SG-4 of FS_0 is recorded higher than SG-1 & SG-2. During loading, the bottom plate moved upward along with frame while the sheathing under compression remains stationary, therefore this phenomenon caused high shear stress concentration between the sheathing and bottom plate and that caused the delamination between bottom plate and sheathing in Fig. 4(a). On the other hand, in FS_{10} due to the stress concentration at anchor bolts, the bottom of RHS plate deformed into transverse splitting of matrix as shown in Fig. 4(g). Overall, reduction in the sheathing length significantly improved the in-plane shear performance of the panel by avoiding premature failure.

3.2. *Effect of wall openings*

The effect of wall opening is evaluated by comparing the FS_{10} (without opening) and $FS_{10}O$ (with opening). The overall results show that the shear stiffness can be estimated from the percentage area removed for the wall opening. The effects of wall opening on load deflection, failure behaviour and load strain behaviour are discussed in the following sections.

3.2.1. *Load deflection behaviour*

In Fig. 7, panels FS_{10} and $FS_{10}O$ exhibit linear behaviour until 6.7 kN and 5.8 kN respectively. The shear stiffness of FS_{10} and $FS_{10}O$ is calculated as 233 N/mm and 152 N/mm respectively from the linear portion of the curves. The 34.7% lower value of experimental shear stiffness of FS_{10} can be explained by the removal of 37.5% area due to the opening in the wall panels, similar reduction is also observed by [28]. However, Shahnewaz et al. [46] proposed that reduction on shear stiffness by wall openings can be calculated by Eq. (3) and the calculated stiffness of $FS_{10}O$ is 177 N/mm which is 14.12% over estimated. This imperfection could be due to the local rotation at wall opening area of panel $FS_{10}O$ in Fig. 7(b), which is also observed in [46,47]. Fig. 7(b) shows linear deflection behaviour of wall panel along panel height until 2100 mm. Thereafter, even at very low load a reduction in deflection can be observed. This indicates that overall panel did not deform uniformly but a local deformation around wall opening area occurred. A linear relation can be observed FS_{10} exhibited a maximum load at 11.6 kN with horizontal deflection of 79.8 mm and $FS_{10}O$ reached at 9.83 kN with horizontal deflection of 105 mm. Both panels exhibit similar linear and non-linear behaviours which are further explained in the following section.

$$K_{Opening} = K_{Full}\left[1 - \frac{r_{o/w}\left(A_o/A_w\right)}{\sqrt{r_{o/w} + r_o\left(A_o/A_w\right)}}\right] \tag{3}$$

where $K_{opening}$ is the shear stiffness of $FS_{10}O$, K_{Full} is the shear stiffness of FS_{10}, r_o is aspect ratio of opening, $r_{o/w}$ is aspect ratio of opening to wall (max. of opening width/wall width or opening height/wall height), A_0 area of opening and A_w area of wall.

3.2.2. *Failure behaviour*

The removal of sheathing area from the panel did not affect the failure behaviour because failure is governed by the bottom plate as discussed in Section 3.1.3. Panel $FS_{10}O$ exhibits a linear elastic behaviour until 5.5 kN load compared with 6.9 kN in FS_{10} and then a cracking sound was heard that could be due to the initiation of cracking of insert in the bottom plate in Fig. 4(i). Thereafter decrease in the shear stiffness can be observed in the panel. At 6.7 kN, a load drop was observed that could be due to the further crushing of insert along with washer inundation in Fig. 4(j). Thereafter the panel sustain the shear stiffness until final failure at 9.8 kN with sudden drop in load and that can be explained by the splitting of bottom RHS plate in Fig. 4(j). The inundation of washer damaged the top portion of

Panel Name	Failure bahaviour of wall panels			
FS_0	 (a) Delamination of sheathing at 6.84 kN	 (b) Corner splitting at 5.66 kN	 (c) Insert crushing at 5.66 kN	 (d) Rivets pull off at 6.01 kN
FS_{10}	 (e) Insert crushing at 6.91 kN and 8.7kN	 (f) Washer inundation at 8.7 kN	 (g) Transverse splitting at 11.66 kN	 (h) End crushing at 11.66 kN
$FS_{10}O$	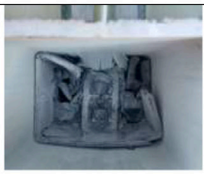 (i) Insert crushing at 5.5 kN	 (j) Washer inundation at 6.7 kN	 (k) Transverse splitting at 9.8 kN	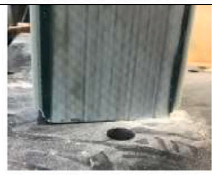 (l) End crushing at 9.8 kN
$FS_{10}B_2$	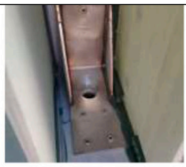 (m) Enlargement of bolt hole at 14.6 kN	 (n) Bending of angle bracket at 14.6 kN	 (o) Isometric view of (n)	 (p) Delamination of sheathing at 14.1 kN
$FS_{10}B_4$	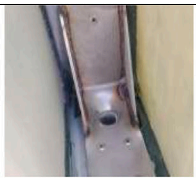 (q) Enlargement of bolt hole at 13.9 kN	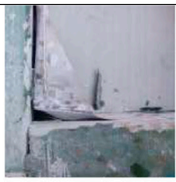 (r) Bending of angle bracket at 13.9 kN	 (s) Isometric view of (n)	 (t) Delamination of sheathing at 15.43 kN
DFS_{10}	 (u) Delamination of sheathing at 20.5 kN	 (v) Bending of angle bracket at 19.5 kN	 (w) Rivets pull off at 19.5 kN	 (y) Rivets pull off at 19.5 kN

Fig. 4. Failure behaviour of wall panels.

Table 3
Summary of the full-scale test of composite wall panels.

Wall panel	Failure load (kN)	Stiffness (N/mm) $K = \frac{\Delta F}{\Delta \delta}$	% Stiffness of panels to FS_{10}	Final failure
FS_0	6.84	229	98.28	Delamination in sheathing at bottom plate
FS_{10}	11.66	233	100	Bottom plate transverse splitting
$FS_{10}O$	9.80	152	65.30	Bottom plate transverse splitting
$FS_{10}B_2$	14.60	392	168.24	Delamination in sheathing at bottom plate
$FS_{10}B_4$	15.43	386	165.66	Delamination in sheathing at bottom plate
DFS_{10}	19.50	1359	583.26	Delamination in sheathing at bottom plate

Specimen designation system.
F (Single frame), DF (Double frame), Sx ($_0$ = full sheathing, $_{10}$ = 10 mm sheathing offset from bottom) O (Window opening), Bx ($_2$ = two customised angle brackets, $_4$ = four customised angle brackets).

bottom RHS plate and intensified the crushing of insert. Thereafter concentrated load is transferred to the bottom portion of RHS plate

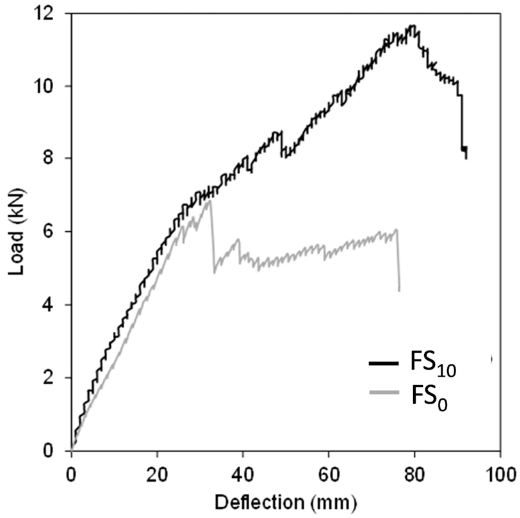

Fig. 5. Load deflection for sheathed wall panels FS_{10} and FS_0.

which caused the final transverse splitting failure. A minor crushing of vertical stud like FS_{10} can also be observed in the panel $FS_{10}O$ in Fig. 4(l). Furthermore, Fig. 7(b) depicts the lateral deflection of wall panel along the height starting from the base of window opening to full height. A drop in deflection at 2100 mm indicates the local deformation in panel explained in Section 3.2.1.

3.2.3. Load strain behaviour

Fig. 8 shows the load strain behaviour of FS_{10} and $FS_{10}O$ wall panels. SG-1 and SG-2 of both panels exhibits linear tensile and compression strain behaviour until the ultimate failure respectively. A significant higher strain in FS_0O indicates that reduction of the sheathing area exerted higher axial strain on the vertical studs. SG-3 and SG-4 of FS_{10} exhibit linear load strain behaviour until the failure with minor fluctuation of SG-4 at 8.1 kN due to the major crushing of insert as explained in Section 3.1.3. Whereas, SG-3 and SG-4 of $FS_{10}O$ are attached near to the bottom plate, therefore strain fluctuations after 5.7 kN can be observed due to the initiation of crushing of inserts. Strain in SG-3 of FS_{10} is recorded higher than $FS_{10}O$, because SG-3 in FS_{10} is placed in the middle of wall panel where the diagonal strain is maximum in sheathing under in-plane shear load. However, RHS studs in FS_0O experienced higher strain compared with $FS_{10,}$ indicating that lower sheathing area provide lower resistance to in-plane shear load. Overall, reduction of sheathing decreases the panel stiffness and loading capacity of the composite wall panel, but with similar failure behaviour, due to the significant lower transverse strength of RHS bottom plate.

3.3. Effect of type of angle brackets

The effect of angle brackets is evaluated by comparing the FS_{10} (with normal brackets), $FS_{10}B_2$ (with two customised brackets) and $FS_{10}B_4$ (with four customised brackets). The overall results show that the customised brackets increased the loading capacity and shear

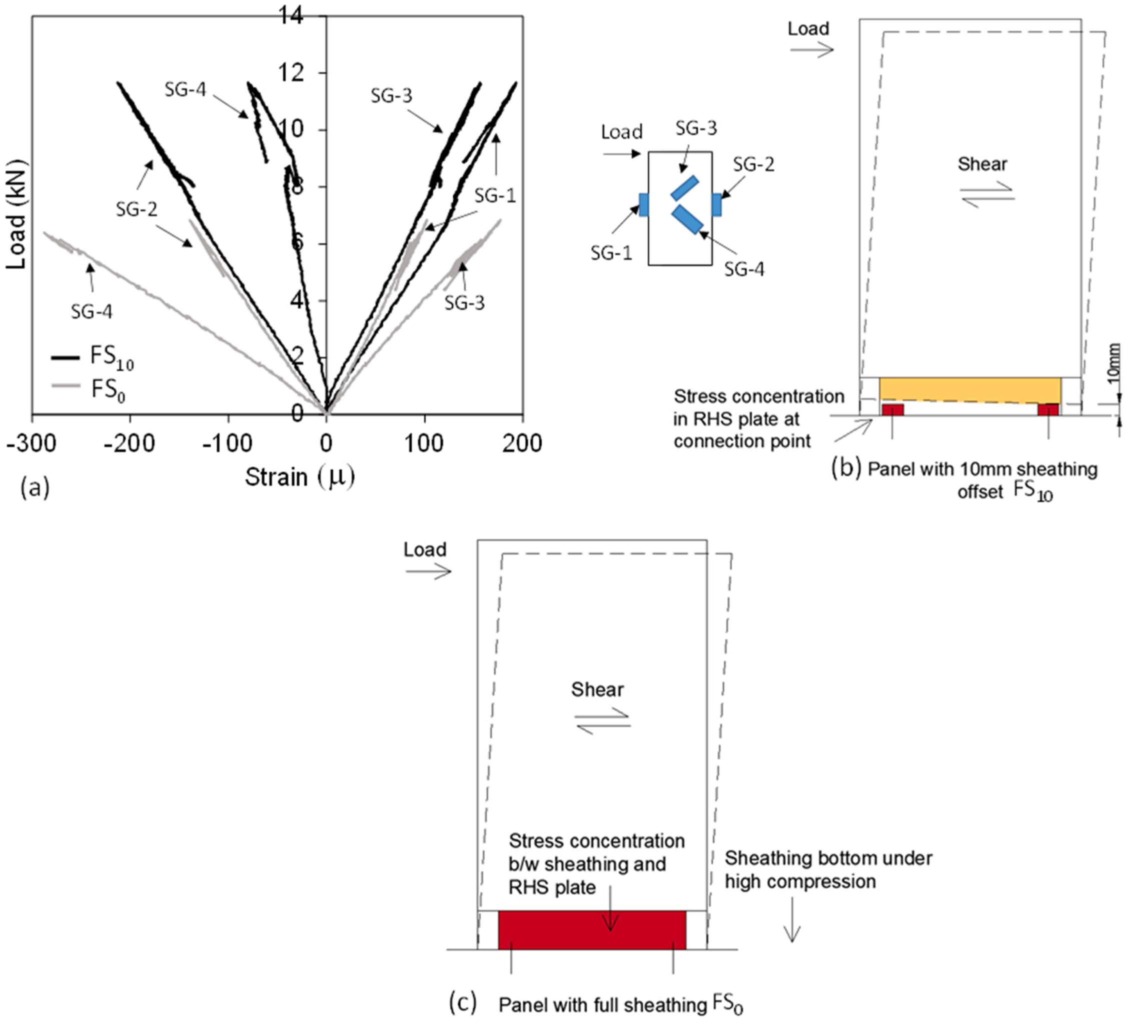

Fig. 6. (a) Load strain behaviour of sheathed wall panels FS_{10} and FS_0 (b) FS_{10} failure mechanism (c) FS_0 failure mechanism.

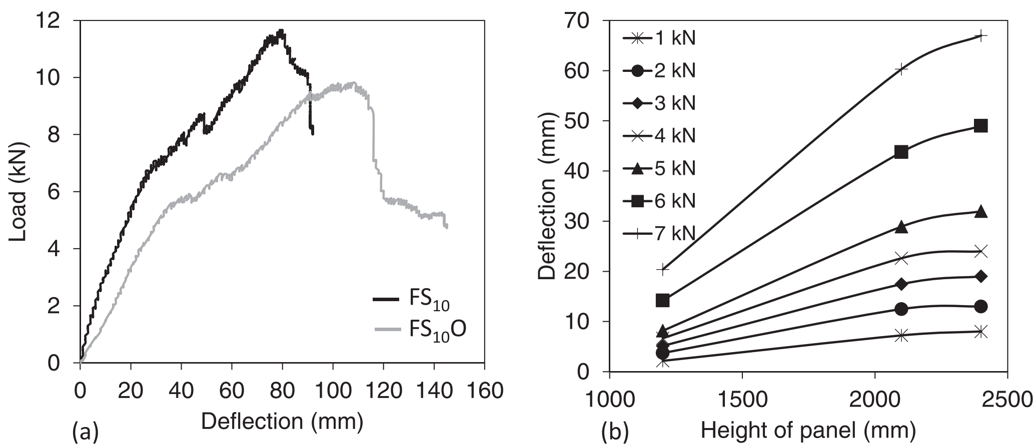

Fig. 7. (a) Load deflection behaviour of FS_{10} and FS_0O wall panels (b) DIC lateral displacement around window opening.

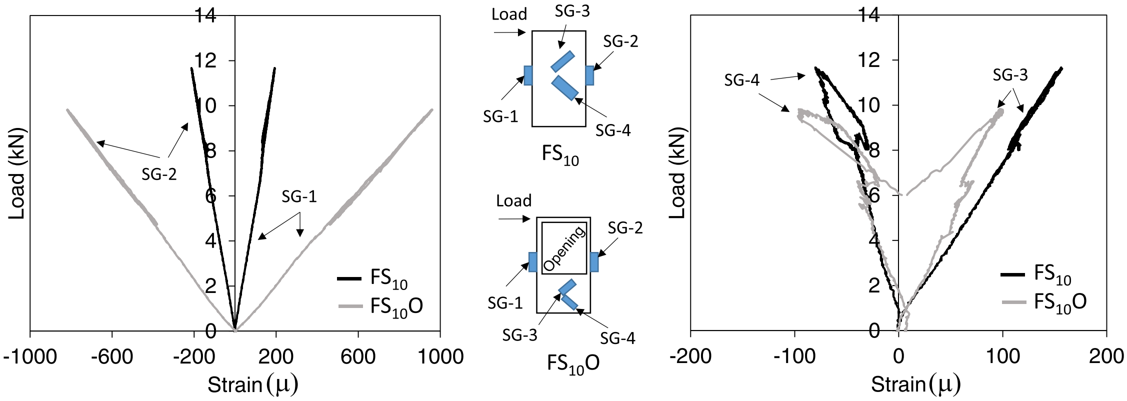

Fig. 8. Load strain behaviour of FS_{10} and FS_0O wall panels.

resistance of the wall panel due to the yielding of bracket before final failure. Whereas, no significant variation is observed by increase of the number of customised brackets, because of the failure behaviour of $FS_{10}B_2$ and $FS_{10}B_4$ governed by bottom load side angle bracket. The effects of fittings on load deflection, failure behaviour and load strain behaviour are discussed in the following sections.

3.3.1. Load deflection behaviour

Fig. 9 shows the load deflection behaviour of panels FS_{10}, $FS_{10}B_2$ and $FS_{10}B_4$. Panels $FS_{10}B_2$ and $FS_{10}B_4$ exhibit linear behaviour until 14.6 kN and 15.43 kN, also with similar shear stiffness of 391 N/mm and 386 N/mm respectively based on the linear portion of the curves. Both panels exhibit similar stiffness and loading capacity but with 1.52 and 1.29 times higher stiffness and loading capacity than FS_{10}, respectively. This indicates that the addition of customised angle brackets can contribute to the overall panel stiffness and loading capacity. However, similar stiffness of $FS_{10}B_2$ and $FS_{10}B_4$ panel can be due to the stiffness provided by only the load side bottom customised bracket. The load on loading side anchor bolt can be calculated by Eq. (4) with the consideration of the rotation of panel at the bottom left corner of the panel in Fig. 3(a). Bottom load side anchor bolt always experiences high reaction due to the applied load and the resulting high stress concentration. Therefore FS_{10}, $FS_{10}B_2$ and $FS_{10}B_4$ panels had similar failure behaviour as further explained in further section.

$$PxH = pxL \tag{4}$$

where P is the load applied, H is the height of the wall panel, p is load on anchor bolt and L is the distance of bolt from edge of wall panel.

3.3.2. Failure behaviour

Panel $FS_{10}B_2$ follows a linear behaviour until 14.6 kN thereafter, a drop in the load can be observed. This could be due to the enlargement of the bolt hole and bending of the angle bracket as shown in Fig. 4(m) and (n) respectively. Upon further loading, the continuous deformation in brackets transferred the load between sheathing and bottom RHS plate. Hence, an instant delamination can be observed in Fig. 4(p) at 14.1 kN. Similarly, for panel $FS_{10}B_4$, a load drop at 13.9 kN was observed and similar failures such as enlargement of bolt hole and bending of angle bracket was observed in Fig. 4(q) and (r) respectively. Finally, the panel $FS_{10}B_4$ failed due to the delamination of bottom plate in Fig. 4(t) at 15.43 kN. Whereas, in contrary to these failures, panel FS_{10} failed due to the transverse cracking in the bottom RHS in Fig. 4(h) plate as discussed in Section 3.1.2. Therefore, the addition of angle brackets in $FS_{10}B_2$ and $FS_{10}B_4$ panels altered the failure behaviour from transverse cracking of the bottom plate to the delamination of sheathing at bottom plate location. This indicates that the addition of angle brackets and insert at hold down location could increase the loading capacity through different failure mechanism. However, failure occurred at the bottom load side anchor bolt as shown in Fig. 4(e), (i), (m) and (q) in all panels. The strain behaviour of $FS_{10}B_2$ and $FS_{10}B_4$ panels are explored further and compared with FS_{10} in following section.

3.3.3. Load strain behaviour

Fig. 10 (a) shows the load strain behaviour of SG-1 and SG-3 of FS_{10}, $FS_{10}B_2$ and $FS_{10}B_4$ panels. SG-1 is attached to the load side of the vertical stud, showing linear tensile behaviour. Similarly, SG-3 is attached on the sheathing, with linear tensile behaviour until final failure. Thereafter, reversion in strain can be observed with decrease in load. The minor strain fluctuations in SG-1 and SG-3 in FS_{10} were due to the local failures as explained in Section 3.1.2. In Fig. 10 (b), SG-2 is attached to the compression studs and follows a linear compression behaviour. Similarly, SG-4 is attached on the sheathing and showed linear compression behaviour until the final failure. Overall, the load strain behaviour indicates that regardless the type and quantity of angle brackets, FS_{10}, $FS_{10}B_2$ and $FS_{10}B_4$ panels have similar trends in terms of stain. $FS_{10}B_2$ and $FS_{10}B_4$ present similar strain level, loading capacity and failure behaviour, highlighting the possibility of use one set of customised angle bracket to achieve high loading capacity.

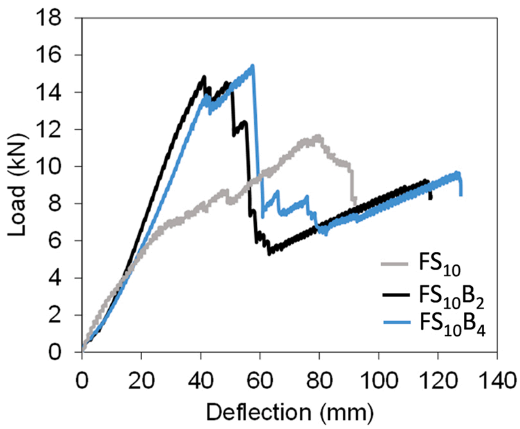

Fig. 9. Load deflection behaviour of FS_{10}, $FS_{10}B_2$ and $FS_{10}B_4$ wall panels.

3.4. Double wall and single wall panel

The effect of wall width is evaluated by comparing DFS_{10} (double wall panel) and $FS_{10}B_2$ (Single wall panel with two customised brackets). The overall results show that double frame has higher panel stiffness but lower loading capacity per unit width. This is due to the high load transfer on load side anchor bolt due to the wider panel.

3.4.1. Load deflection behaviour

In Fig. 11 (a), panels DFS_{10} exhibits linear behaviour until 20.5 kN corresponding to a horizontal deflection of 19.8 mm. Then a sudden drop of 67% load was observed due to the initial failure explained in following section. Thereafter a linear increment in load was observed due to the load carried by angle brackets until final failure at 19.5 kN and 92 mm horizontal deflection. Whereas, $FS_{10}B_2$ presents loading capacity of 15.2 kN with a horizontal deflection of 58.1 mm. Fig. 11 (b) shows the normalised loading capacity of both panels by dividing the width of the wall panel. It is clear from the graph that the normalised loading capacity of single wall panel is higher than the double wall because higher panel width exerts higher load on the load side hold-down bolt. Whereas, double panel exhibits 2.6 times higher shear stiffness than single panel as shown in Fig. 11 (b). Because single panel $FS_{10}B_2$ has high aspect ratio of 4:1 (height:width ratio) and has a tendency to deform under the rigid body rotation as explained by [48]. The failure behaviour of such panels is further explained in the following sections.

3.4.2. Failure behaviour

Panel DFS_{10} follows a linear behaviour until 20.5 kN; thereafter, a significant drop in the load can be observed. This was due to the delamination of bottom RHS plate in Fig. 4(u). At 26 mm deflection, the panel started regaining the load because even after the delamination of bottom plate in Fig. 4(u), the hold-down contributed in carrying the load until reaching 19.5 kN load with lateral deflection of 75 mm. Thereafter until 92 mm no load increment was observed, indicating the yielding in rivets, and causing the final failure due to the rivets pulled off from the vertical plate in loading side and from the bottom of normal bracket in compression side of panel (as shown in Fig. 4(w) and (y) respectively). $FS_{10}B_2$ also shows the similar failure behaviour except of rivet pull off as discussed in Section 3.3.2. The load strain behaviour of both panels is discussed in the following section.

3.4.3. Load strain behaviour

Fig. 12, presented the load strain behaviour of DFS_{10} and $FS_{10}B_2$ wall panels. SG-1, SG-3 and SG-5 presented linear tensile behaviour and SG-2, SG-4 and SG-6 presented linear compression behaviour until final failure. SG-1 shows 2.7 times higher tensile strain in $FS_{10}B_2$ than DFS_{10}, supporting the reduction of stiffness at similar level of 2.6 times as discussed in Section 3.4.1. Whereas SG-2, SG-3 and SG-4 showed 1.6, 1.9 and 2.9 times higher strain in $FS_{10}B_2$ than DFS_{10}. Such variations could be due to the location of strain measurements as a result of variation in width of both panels. However, in panel DFS_{10} higher strain in SG-5 than SG-3 can be explained as the second panel P-2 in Fig. 12 provided lateral movement resistance to first panel P-1. Therefore, lower displacement exhibits lower strain in SG-3 of P-1. Similarly, SG-4 recorded lower strain than SG-6 in panel DFS_{10}.

4. Conclusion

The structural performance of composite wall panels under in-plane shear load was evaluated in this paper. The effects of sheathing height offset, presence of wall opening, types of angle brackets at frame corners and number of wall panel (single and double) were clarified. Based on the experimental investigation, the following conclusions can be drawn.

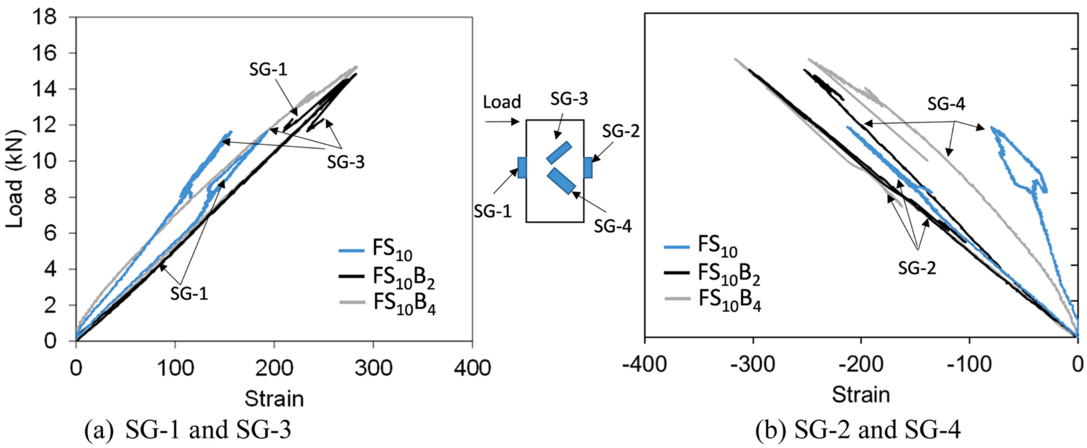

Fig. 10. Load strain behaviour of FS_{10}, $FS_{10}B_2$ and $FS_{10}B_4$ wall panels.

- The sheathing offset (10 mm from the bottom) enhanced the loading capacity of the composite wall panel as it avoided the additional compression stress in the sheathing and transferred most of the load to the pultruded FRP sections. Panels with full sheathing experienced stress concentration resulting in premature delamination failure at the bottom plate. No variation on shear stiffness was observed in both sheathing configuration.
- The presence of window opening reduced the loading capacity and shear stiffness of the composite wall panel. The decrease in strength and stiffness is directly proportional to the ratio of wall opening to total area of the wall. This can be reliably calculated by the empirical formula considering the aspect ratio of window opening to wall modules.
- The provision of customised angle brackets at the corners of FRP frame increased the loading capacity and stiffness of composite wall systems. However, the number of customised brackets has insignificant effect on the loading capacity, stiffness and failure behaviour. Two customised brackets provided in diagonal corners are sufficient in improving the in-plane shear behaviour.
- The loading capacity per unit width of single panel is marginally higher than the double wall panel. The stiffness of double wall is 2.6 times higher than the single wall panel, because of its tendency to deflect with higher deflection caused by rigid body rotation.

The experimental results obtained from this study indicates that composite wall system may be considered as an alternative material for modular construction. However, a detailed comparative study between GFRP composite and other conventional material wall system should be considered for future research. A careful attention should however be given to the fabrication of wall panels and connection details to maximise the utilisation of high strength properties of the GFRP materials.

CRediT authorship contribution statement

Arvind Sharda: Conceptualization, Methodology, Data curation, Formal analysis, Investigation, Validation, Writing – original draft. **Allan Manalo:** Conceptualization, Methodology, Supervision, Writing – review & editing. **Wahid Ferdous:** Supervision, Methodology, Writing – review & editing. **Yu Bai:** Methodology, Writing – review & editing. **Lachlan Nicol:** Writing – review &

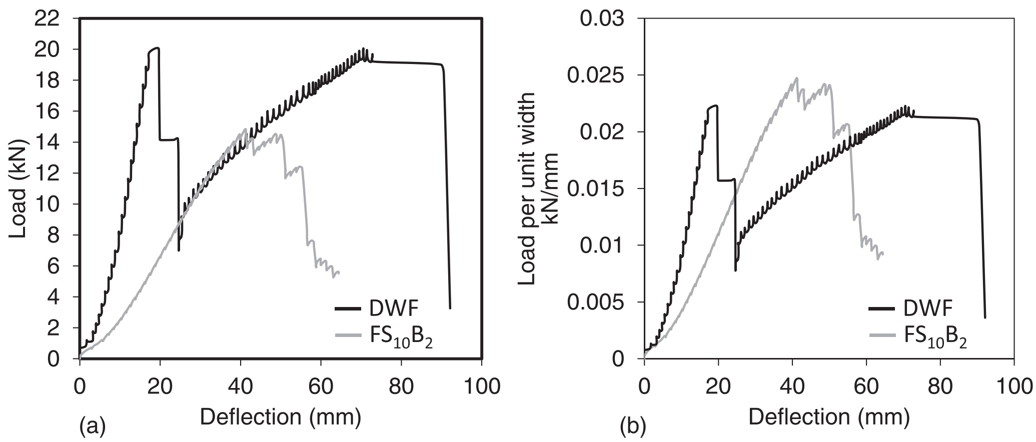

Fig. 11. DWF and $FS_{10}B_2$ wall panels (a) Load deflection behaviour (b) Normalised load with panel width vs deflection of panel.

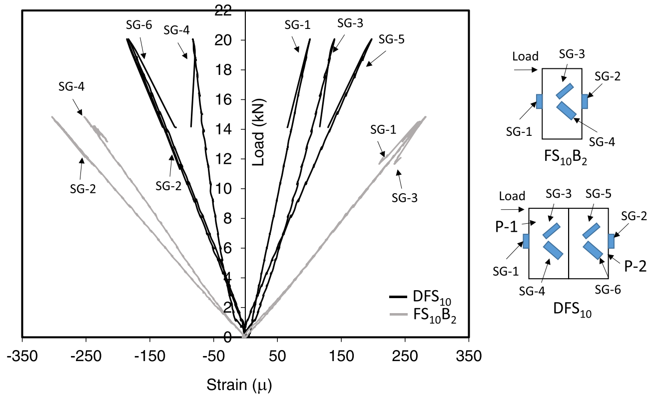

Fig. 12. Load strain behaviour of DFS_{10} and $FS_{10}B_2$ wall panels.

editing. **Ali Mohammed:** Writing – review & editing. **Brahim Benmokrane**: Writing – review & editing.

Declaration of Competing Interest

The authors declare that they have no known competing financial interests or personal relationships that could have appeared to influence the work reported in this paper.

Data availability

Data will be made available on request.

Acknowledgements

The authors wish to acknowledge the support of the Australian Research Council through the Discovery Scheme (DP180102208) and the Natural Sciences and Engineering Research Council of Canada (NSERC). The authors are also grateful to Wagners Composite Fibre Technology for providing the composite wall specimens and to the Centre of Future Materials (CFM) for the facilities.

References

[1] W. Ferdous, Y. Bai, T.D. Ngo, A. Manalo, P. Mendis, New advancements, challenges and opportunities of multi-storey modular buildings–a state-of-the-art review, Eng. Struct. 183 (2019) 883–893.
[2] K. Kabirifar, M. Mojtahedi, C. Wang, V.W.Y. Tam, Construction and demolition waste management contributing factors coupled with reduce, reuse, and recycle strategies for effective waste management: a review, J. Clean. Prod. 263 (2020), 121265.
[3] V.W. Tam, C.M. Tam, S. Zeng, W.C. Ng, Towards adoption of prefabrication in construction, Build. Environ. 42 (10) (2007) 3642–3654.
[4] F. Innella, M. Arashpour, Y. Bai, Lean methodologies and techniques for modular construction: chronological and critical review, J. Constr. Eng. Manag. 145 (12) (2019), 04019076.
[5] W. Ferdous, A. Manalo, A. Sharda, Y. Bai, T.D. Ngo, P. Mendis, Construction industry transformation through modular methods, Innov. Constr. (2022) 259–276.
[6] T. Keller, N.A. Theodorou, A.P. Vassilopoulos, J. De, Castro, Effect of natural weathering on durability of pultruded glass fiber–reinforced bridge and building structures, J. Compos. Constr. 20 (1) (2016), 04015025.
[7] J. Correia, S. Cabral-Fonseca, F. Branco, J. Ferreira, M. Eusébio, M. Rodrigues, Durability of pultruded glass-fiber-reinforced polyester profiles for structural applications, Mech. Compos. Mater. 42 (4) (2006) 325–338.
[8] Z. Aljazaeri, Z. Al-Jaberi, Numerical study on flexural behavior of concrete beams strengthened with fiber reinforced cementitious matrix considering different concrete compressive strength and steel reinforcement ratio, Int. J. Eng. 34 (4) (2021) 793–802.
[9] M.K. Askar, A.F. Hassan, Y.S.S. Al-Kamaki, Flexural and shear strengthening of reinforced concrete beams using FRP composites: a state of the art, Case Stud. Constr. Mater. 17 (2022), e01189.
[10] Z.K. Aljaberi, J.J. Myers, M. ElGawady, A comparative study of flexural behavior of reinforced masonry walls strengthened with near-surface mounted FRP bars or externally bonded FRP sheets. Insights and Innovations in Structural Engineering, Mechanics and Computation, CRC Press, 2016, pp. 1459–1464.
[11] M. El-Diasity, H. Okail, O. Kamal, M. Said, Structural performance of confined masonry walls retrofitted using ferrocement and GFRP under in-plane cyclic loading, Eng. Struct. 94 (2015) 54–69.
[12] A.A. Mohammed, A.C. Manalo, W. Ferdous, Y. Zhuge, P.V. Vijay, A.Q. Alkinani, A. Fam, State-of-the-art of prefabricated FRP composite jackets for structural repair, Eng. Sci. Technol. Int. J. 23 (5) (2020) 1244–1258.
[13] O.F. Otoom, W. Lokuge, W. Karunasena, A.C. Manalo, T. Ozbakkaloglu, D. Thambiratnam, Experimental and numerical evaluation of the compression behaviour of GFRP-wrapped infill materials, Case Stud. Constr. Mater. 15 (2021), e00654.
[14] A. Sharda, A. Manalo, W. Ferdous, Y. Bai, L. Nicol, A. Mohammed, B. Benmokrane, Axial compression behaviour of all-composite modular wall system, Compos. Struct. 268 (2021), 113986.
[15] X. Lei, Q. Yujun, B. Yu, Q. Chengyu, W. Hao, F. Hai, Z. Xiao-Ling, Sandwich assemblies of composites square hollow sections and thin-walled panels in compression, Thin-Walled Struct. 145 (2019), 106412.
[16] S. Satasivam, Y. Bai, Mechanical performance of bolted modular GFRP composite sandwich structures using standard and blind bolts, Compos. Struct. 117 (2014) 59–70.
[17] S. Satasivam, Y. Bai, Mechanical performance of modular FRP-steel composite beams for building construction, Mater. Struct. 49 (10) (2016) 4113–4129.
[18] S. Satasivam, Y. Bai, Y. Yang, L. Zhu, X.-L. Zhao, Mechanical performance of two-way modular FRP sandwich slabs, Compos. Struct. 184 (2018) 904–916.

[19] F. Zhang, W. Liu, Z. Ling, H. Fang, D. Jin, Mechanical performance of GFRP-profiled steel sheeting composite sandwich beams in four-point bending, Compos. Struct. 206 (2018) 921–932.
[20] A. Manalo, Structural behaviour of a prefabricated composite wall system made from rigid polyurethane foam and magnesium oxide board, Constr. Build. Mater. 41 (2013) 642–653.
[21] J.M. Branco, F.T. Matos, P.B. Lourenço, Experimental in-plane evaluation of light timber walls panels, Buildings 7 (3) (2017) 63.
[22] Y. Xiao, Z. Li, R. Wang, Lateral loading behaviors of lightweight wood-frame shear walls with ply-bamboo sheathing panels, J. Struct. Eng. 141 (3) (2015), B4014004.
[23] A. Lafontaine, Z. Chen, G. Doudak, Y.H. Chui, Lateral behavior of light wood-frame shear walls with gypsum wall board, J. Struct. Eng. 143 (8) (2017), 04017069.
[24] E. Yüksel, A. Güllü, H. Özkaynak, C. Soydan, A. Khajehdehi, E. Şenol, A.M. Saghayesh, H. Saruhan, Experimental investigation and pseudoelastic truss model for in-plane behavior of corrugated sandwich panels with polyurethane foam core. Structures, Elsevier, 2021, pp. 823–842.
[25] J.-J. Wang, X. Nie, F.-M. Bu, M.-X. Tao, J.-S. Fan, Experimental study and design method of shear-dominated composite plate shear walls, Eng. Struct. 215 (2020), 110656.
[26] J. Mo, B. Uy, D. Li, H.-T. Thai, H. Tran, A review of the behaviour and design of steel–concrete composite shear walls. Structures, Elsevier, 2021, pp. 1230–1253.
[27] M. Seddighi, M.A. Barkhordari, S. Hosseinzadeh, The wall–frame interaction in composite FRP-steel plate shear walls, Iran. J. Sci. Technol. Trans. Civ. Eng. 46 (1) (2022) 133–156.
[28] Ö. Anil, A. Togay, Ü. Karagöz Işleyen, C. Söğütlü, N. Döngel, Hysteretic behavior of timber framed shear wall with openings, Constr. Build. Mater. 116 (2016) 203–215.
[29] L. Kuai, S. Ormarsson, J. Vessby, R. Maharjan, A numerical and experimental investigation of non-linear deformation behaviours in light-frame timber walls, Eng. Struct. 252 (2022), 113599.
[30] D. Casagrande, R. Fanti, G. Doudak, A. Polastri, Experimental and numerical study on the mechanical behaviour of CLT shearwalls with openings, Constr. Build. Mater. 298 (2021), 123858.
[31] M. Mosoarca, Failure analysis of RC shear walls with staggered openings under seismic loads, Eng. Fail. Anal. 41 (2014) 48–64.
[32] X. Zhai, X. Zhang, C. Cao, W. Hu, Study on seismic performance of precast fabricated RC shear wall with opening filling, Constr. Build. Mater. 214 (2019) 539–556.
[33] M. Husain, A.S. Eisa, M.M. Hegazy, Strengthening of reinforced concrete shear walls with openings using carbon fiber-reinforced polymers, Int. J. Adv. Struct. Eng. 11 (2) (2019) 129–150.
[34] H. Wu, A. Chen, S. Laflamme, Seismic behavior of glass fiber-reinforced polymer wall panels, Compos. Struct. 203 (2018) 300–309.
[35] A. Sharda, A. Manalo, W. Ferdous, Y. Bai, L. Nicol, A. Mohammed, B. Benmokrane, Flexural behaviour of composite modular wall systems under uniformly distributed and concentrated loads, Compos. Struct. 303 (2023), 116346.
[36] L. Pozza, R. Scotta, D. Trutalli, M. Pinna, A. Polastri, P. Bertoni, Experimental and numerical analyses of new massive wooden shear-wall systems, Buildings 4 (3) (2014) 355–374.
[37] R.M. Hizam, A.C. Manalo, W. Karunasena, Y. Bai, Behaviour of pultruded GFRP truss system connected using through-bolt with mechanical insert, Compos. Part B Eng. 168 (2019) 44–57.
[38] I. 527-1, Plastics–Determination of Tensile Properties–part 1: General Principles, ISO Geneva, Switzerland, 2012.
[39] O.Id Normalización, ISO 14125: Fibre-reinforced Plastic Composites: Determination of Flexural Properties, ISO1998.
[40] A. International, ASTM D5379/D5379M-12-Standard Test Method for Shear Properties of Composite Materials by the V-Notched Beam Method, ASTM International West Conshohocken, 2012.
[41] ASTM, D2344/D2344M-16, Standard Test Method for Short-Beam Strength of Polymer Matrix Composite Materials and Their Laminates, 2016.
[42] A. Manalo, H. Mutsuyoshi, Behavior of fiber-reinforced composite beams with mechanical joints, J. Compos. Mater. 46 (4) (2012) 483–496.
[43] W.C.F. Technologies, Product Guide, 2021, 2022. ⟨https://www.wagner.com.au/main/what-we-do/composite-fibre-technologies/downloads/technical-guides/⟩.
[44] ASTM-E72-05, Standard Test Methods of Conducting Strength Tests of Panels for Building Construction, ASTM International, 2010.
[45] M.N. Olabi, N. Caglar, M.H. Kisa, S.B. Yuksel, Numerical study on the response of composite shear walls with steel sheets under cyclic loading, J. Build. Eng. 34 (2021), 102069.
[46] I. Shahnewaz, T. Tannert, M. Shahria Alam, M. Popovski, In-plane stiffness of cross-laminated timber panels with openings, Struct. Eng. Int. 27 (2) (2017) 217–223.
[47] M. Mestar, G. Doudak, A. Polastri, D. Casagrande, Investigating the kinematic modes of CLT shear-walls with openings, Eng. Struct. 228 (2021), 111475.
[48] A.J. Salenikovich, J.D. Dolan, The racking performance of shear walls with various aspect ratios. Part 1. Monotonic tests of fully anchored walls, For. Prod. J. 53 (10) (2003) 65–73.